

# Mapping of Local Lattice Orientations and Strains in Epitaxial Oxide Films by Using X-ray Microdiffraction

J. D. Budai, W. Yang, B. C. Larson, J. Z. Tischler, G. E. Ice, W. J. Liu  
Oak Ridge National Laboratory, Oak Ridge, TN, U.S.A

## Introduction

The ability to understand and control the size and orientation of crystallographic grains (i.e., texture) plays an essential role in determining material properties in many technological applications. For example, in high- $T_c$  superconductors such as YBaCuO, high-angle grain boundaries act as weak links, reducing current-carrying capabilities by orders of magnitude. Thus, a significant amount of research in the past decade has focused on developing techniques for fabricating long lengths of highly textured YBaCuO.

Two principal approaches have been considered for producing high-current superconducting wires by using epitaxial deposition of YBaCuO on biaxially textured substrates. In the first approach, a polycrystal metal tape is coated with an oxide buffer layer in which texture is induced by using ion-beam-assisted deposition (IBAD) [1]. A second approach for achieving texture in YBaCuO involves crystallographic alignment induced by the heteroepitaxial growth on rolling-assisted biaxially textured substrates (RABiTS) [2, 3]. In this approach, metal foils (typically Ni) are rolled and annealed to produce  $\{001\}<100>$  cube texture with a mosaic spread of the order  $7^\circ$  full width at half-maximum (FWHM). Epitaxial oxide buffer films and YBaCuO are then grown by pulsed laser deposition (PLD) or another film technique. Suitable epitaxial buffer layers such as  $\text{CeO}_2$  and yttria-stabilized zirconia (YSZ) are required to prevent unwanted chemical reactions, thermal cracking, and delamination in the oxide layers. Both of these approaches have produced short samples with high current densities  $J_c$  of  $>10^6 \text{ A/cm}^2$ . However, fundamental materials processing issues such as texture development, interdiffusion, and strain must be addressed before long lengths of high- $J_c$  superconducting wire can be reproducibly produced.

## Methods and Materials

We have investigated the epitaxial growth of oxide buffer-layer films on highly textured RABiTS substrates by using white-beam x-ray Laue microdiffraction techniques at the insertion device (ID) beamlines of the Michigan-Howard-Lucent Technologies-Bell Labs Collaborative Access Team (MHATT-CAT) and University-National Laboratory-Industry CAT (UNI-CAT) at APS. A pair of elliptical Kirkpatrick-Baez mirrors are used to focus the undulator radiation to beam diameters of  $\sim 0.5$  to  $1 \mu\text{m}$  [4]. The sample is scanned by using a high-precision Newport PM500 linear translation stage with

$0.05\text{-}\mu\text{m}$  repeatability. A charge-coupled device (CCD) area detector records the spatially resolved Laue patterns at each sample position. Peaks are located, and the patterns are subsequently analyzed with an automated indexing program [5-7]. The output is the local lattice orientation matrix and deviatoric strain tensor for each layer of the multilayer samples. By step-scanning the sample, the microbeam Laue method yields a large-area, real-space map of the local crystallographic orientation. For a thin film, this information is similar to orientation imaging microscopy (OIM) by using electron backscatter diffraction (EBSD). However, the x-ray penetration is much greater than the electron penetration, enabling the simultaneous, nondestructive mapping of all layers of multilayer RABiTS samples with high angular resolution ( $\sim 0.01^\circ$ ). Materials issues being studied by microbeam diffraction include: the effects of processing conditions such as substrate temperature; the effect of substrate grooving near grain boundaries; and comparisons of different film deposition techniques.

## Results

Figure 1 shows (001) x-ray microbeam orientation maps of a RABiTS sample from both the textured Ni substrate (Fig. 1a) and a PLD-deposited  $\text{CeO}_2/\text{YSZ}$  buffer layer (Fig. 1b). In these maps, the angular deviation of the [001] direction away from the surface normal is indicated for each spatial position by a color from the key with a  $0\text{-}5.3^\circ$  range. A  $0.72 \times 0.72\text{-mm}$  area was scanned with an  $8\text{-}\mu\text{m}$  step size. The data for constructing these maps were collected in about 15 h; however, x-ray exposures accounted for less than less than 2 h, with the remaining time caused primarily by slow CCD readout. Thus, faster detectors will enable significantly more rapid mapping.

Figure 2 shows the same data presented as pole-figure representations. In this view, the orientation of each pixel is used to generate a discrete point on stereographic projections. Thus, spatial information is absent, but angular distributions may be more easily visualized. As expected, the substrate is observed to be highly  $\{001\}<100>$  textured, and the buffer layer appears approximately epitaxial, with a  $45^\circ$  in-plane relative rotation. It is also apparent in the zoomed figures (radius  $5.3^\circ$  around the normal) that the angular spread within individual Ni grains is smaller than the spread for the corresponding  $\text{CeO}_2/\text{YSZ}$  grains. In other words, the intragrain mosaic in the film is significantly larger than it is in the substrate, consistent with multiple oxide

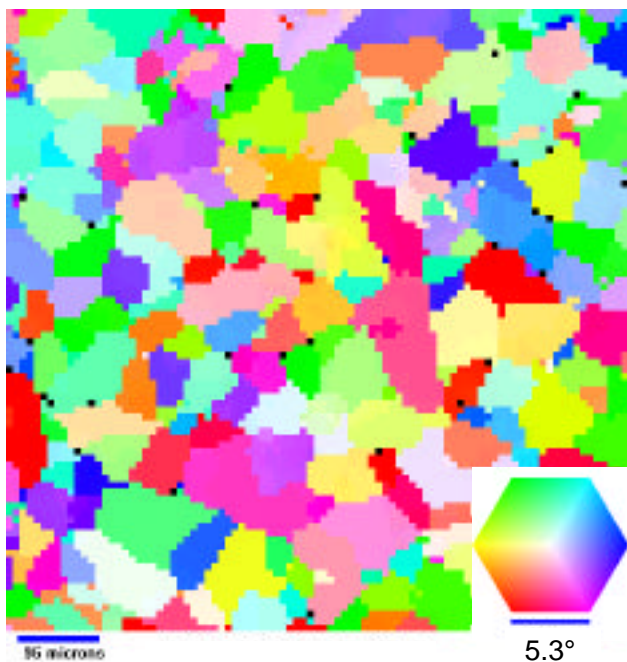


FIG. 1a. Orientation map of textured Ni(001) substrate in a RABiTS sample. Color key in lower right corner.



FIG. 1b. Orientation map of CeO<sub>2</sub>/YSZ oxide buffer layer grown epitaxially in the same RABiTS sample.

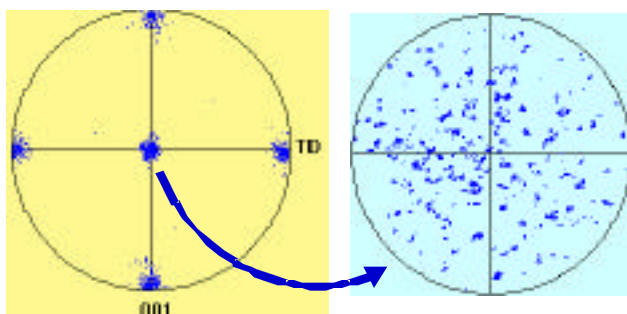


FIG. 2a. Discrete (001) pole figure from the Ni substrate. The radius of the left circle is 90°, and the radius of the zoom on the right is 5.3°.

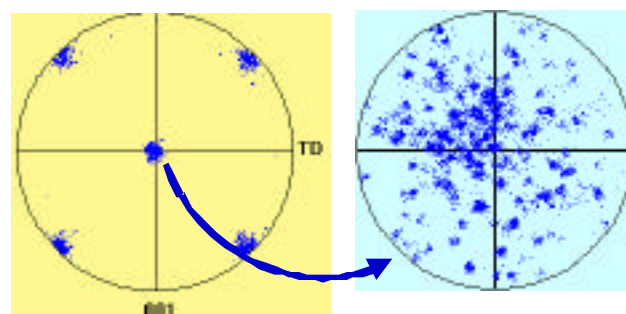


FIG. 2b. Discrete (001) pole figure from the CeO<sub>2</sub>/YSZ oxide buffer layer in the same RABiTS sample.

nucleation sites on each Ni grain. Note that only the out-of-plane orientation information is displayed here by using the (001) poles. Since the microbeam Laue technique provides a complete 3-D orientation matrix at each position, similar orientation maps and discrete pole-figure representations can be constructed to visualize any texture component.

The grain structure and the near-epitaxial relation between the layers are clearly observed in these figures. However, quantitative comparisons for samples grown under a variety of conditions show that the film orientation is generally not exactly aligned with the substrate; rather, the buffer [001] axis exhibits a

crystallographic tilt toward the surface normal with respect to the underlying Ni layer. Thus the colors for corresponding grains in Figs. 1a and 1b are not identical. For samples grown at elevated substrate temperatures in the usual range of 600°-800°C, the tilt angle generally increases linearly with the miscut angle for a particular vicinal Ni grain. In this case, the observed crystallographic tilting is consistent with a ledge growth model [8]. For buffer films grown at a lower temperature (450°C), almost no tilting is observed, revealing the kinetic suppression of ledge flow and the transition to island growth on surface terraces. YBaCuO films grown by PLD on the buffer layers also exhibit crystallographic tilting of the [001] axis toward the surface normal.

AFM measurements have shown that thermal grooving of the Ni substrate foils occurs at grain boundaries when they are annealed for texture development [9]. However, the effect of substrate grooving on subsequent epitaxy and transport properties in RABiTS samples is not known. A particular concern is that local film tilts caused by grooving could disrupt electrical transport across boundary regions. To investigate this concern, microdiffraction measurements from the sample shown in Fig. 1 were obtained with 1- $\mu\text{m}$  step size in the vicinity of a large number of grain boundaries. In all cases, the film orientation changed abruptly at the boundary, and no additional tilting due to substrate grooving was observed.

Films in the initial studies of the RABiTS technique were typically grown by PLD [3]. More recent research has investigated alternative deposition techniques that may enable the practical fabrication of large-area or long-length superconductors. For example, in the *ex situ* “BaF<sub>2</sub> process,” amorphous precursors are deposited at low temperature and then reacted in water vapor at higher temperatures to form epitaxial YBaCuO [10] during solid-phase growth. X-ray microbeam diffraction measurements of RABiTS samples produced by using the BaF<sub>2</sub> process reveal YBaCuO [001] crystallographic tilts in random directions over distances of only a few micrometers. In contrast, the [001] axis for PLD samples is always observed to tilt toward the sample normal. Thus, the local (micrometer-range) YBaCuO mosaic spread is much larger in BaF<sub>2</sub> samples, even though the macroscopic angular spread is comparable to the spread observed in PLD samples. These observations indicate that the YBaCuO films in BaF<sub>2</sub> samples nucleate independently at many nearby locations and do not grow by ledge flow.

## Discussion

The ability to simultaneously map the orientations of the substrate and film layers with micrometer resolution in RABiTS samples yields important insight into the growth mechanisms and the resulting microstructures in these complex epitaxial systems. To our knowledge, these results provide the first observation of systematic crystallographic tilts in a metal-oxide heteroepitaxial system. Further, the quantitative orientation maps enable accurate structural models for developing an understanding of the transport properties of these superconducting materials. The detailed comparison of films grown by PLD with those produced by the BaF<sub>2</sub>

process aids in understanding the differences in the physical properties for films produced by these two techniques. More generally, this study of heteroepitaxial growth illustrates a new materials characterization capability for obtaining local structural and strain information that is applicable to a wide range of thin-film and multilayer systems.

## Acknowledgments

This research was sponsored by the Division of Materials Sciences, U.S. Department of Energy (DOE), under Contract No. DE-AC05-00OR22725 with UT-Battelle, LLC. Experiments were performed at the MHATT-CAT and UNI-CAT beamlines, which are funded by the DOE Office of Science, Office of Basic Energy Sciences (BES). Use of the APS was supported by the DOE BES under Contract No. W-31-109-ENG-38.

## References

- [1] X. D. Wu, S. R. Foltyn, P. N. Arendt, W. R. Blumenthal, I. H. Campbell, J. D. Cotton, J. Y. Coulter, W. L. Hulst, M. P. Maley, H. F. Safar, and J. L. Smith, *App. Phys. Lett.* **67**, 2397-2399 (1995).
- [2] J. D. Budai, R. T. Young, and B. S. Chao, *Appl. Phys. Lett.* **62**, 1836-1838 (1993).
- [3] D. P. Norton, A. Goyal, J. D. Budai, D. Christen, D. Kroeger, E. D. Specht, Q. He, B. Saffian, M. Paranthaman, C. Klabunde, D. Lee, B. Sales, and F. List, *Science* **274**, 755-757 (1996).
- [4] G. E. Ice, J. S. Chung, J. Z. Tischler, A. Lunt, and L. Assoufid, *Rev. Sci. Instrum.* **71**, 2635-2639 (2000).
- [5] G. E. Ice and B. C. Larson, *Adv. Engineering Mater.* **2**, 643-646 (2000).
- [6] J. S. Chung and G. E. Ice, *J. Appl. Phys.* **86**, 5249-5256 (1999).
- [7] B. C. Larson, W. Yang, G. E. Ice, J. D. Budai, and J. Z. Tischler, *Nature* **415**, 887-890 (2002).
- [8] H. Nagai, *J. Appl. Phys.* **45**, 3789-3794 (1974).
- [9] T. G. Truchan, F. H. Rountree, M. T. Lanagan, S. M. McClellan, D. J. Miller, K. C. Goretta, M. Tomsic, and R. Foley, *IEEE Trans. Appl. Supercond.* **10**, 1130-1133 (2000).
- [10] V. F. Solovpov, H. J. Wiesmann, L. J. Wu, M. Suenaga, and R. Feenstra, *IEEE Trans. Appl. Supercond.* **9**, 1467-1470 (1999).